# A Conformational Change in the "Loop E-like" Motif of the Hairpin Ribozyme Is Coincidental with Domain Docking and Is Essential for Catalysis†

Ken J. Hampel and John M. Burke*

*Department of Microbiology and Molecular Genetics, University of Vermont, Burlington, Vermont 05405*

*Received December 14, 2000; Revised Manuscript Received January 24, 2001*

ABSTRACT: The catalysis of site-specific RNA cleavage and ligation by the hairpin ribozyme requires the formation of a tertiary interaction between two independently folded internal loop domains, A and B. Within the B domain, a tertiary structure has been identified, known as the loop E motif, that has been observed in many naturally occurring RNAs. One characteristic of this motif is a partial cross-strand stack of a G residue on a U residue. In a few cases, including loop B of the hairpin ribozyme, this unusual arrangement gives rise to photoreactivity. In the hairpin, G21 and U42 can be UV cross-linked. Here we show that docking of the two domains correlates very strongly with a loss of UV reactivity of these bases. The rate of the loss of photoreactivity during folding is in close agreement with the kinetics of interdomain docking as determined by hydroxyl-radical footprinting and fluorescence resonance energy transfer (FRET). Fixing the structure of the complex in the cross-linked form results in an inability of the two domains to dock and catalyze the cleavage reaction, suggesting that the conformational change is essential for catalysis.

RNA folding is complicated by the ability of any primary sequence to fold into more than one stable conformation, through formation of alternative secondary or tertiary structures (*1*−*4*). Since function is closely linked with structure, usually only one of the alternative conformations retains biological activity. Identifying specific structural rearrangements and learning how they fit into the folding pathway of functional RNAs are, therefore, important goals for those who study RNA biochemistry.

The hairpin ribozyme catalyzes site-specific RNA cleavage and ligation reactions (*5*−*7*). The cleavage reaction yields 2′,3′-cyclic phosphate and 5′-OH termini, and the ligation reaction produces a phosphodiester linkage from these termini. The minimal ribozyme−substrate complex that retains catalytic ability is composed of two domains, A and B (Figure 1) (*8*). The A domain contains a small symmetrical internal loop flanked by two short Watson−Crick helices, and contains the site of cleavage and ligation. The B domain is composed of a larger, asymmetric internal loop that contains many of the conserved bases and important nucleotide functional groups, suggesting that an interaction between the two domains is important for activity (*6*, *7*). Domain separation experiments and circular permutation of the minimal catalytic motif have been used to demonstrate an essential tertiary interaction between the two domains (*9*−*11*). In the native form, the two catalytic domains are separated by a four-way helical junction. The orientation of the helices from this junction directs the interaction between the two domains (*12*).

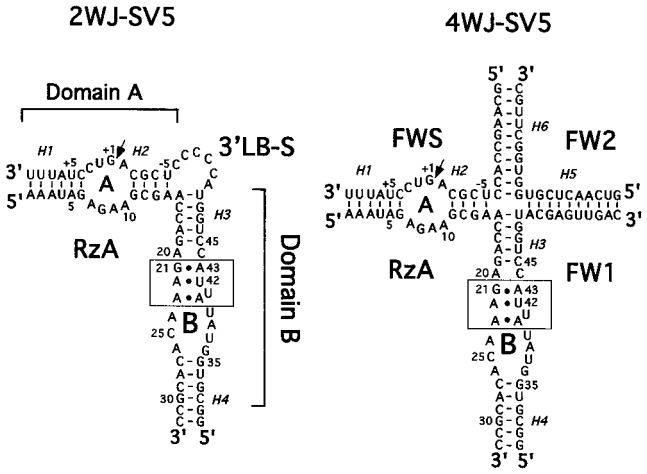


FIGURE 1: Secondary structures of the minimal two-way helical junction (2WJ-SV5), and native four-way helical junction (4WJ-SV5), hairpin ribozyme−substrate constructs used in this study. The UV reactive subdomain of loop B is enclosed in a box. The site of cleavage is indicated with an arrow.

The A and B domains separately form stable tertiary structures that have been determined at high resolution by NMR[1] spectroscopy (*13*, *14*). The structure of loop B features a photoreactive substructure, termed the loop E motif, comprised of three noncanonical base pairs and a bulged U (*14*). A striking characteristic of the motif is cross-strand stacking of two bases, G21 and U42, and this tertiary structure element gives rise to observable hypersensitivity to UV irradiation (*15*, *44*). The sequence which forms this tertiary fold was first observed within internal loops of the

† This work was supported by a grant from the National Institutes of Health (Grant AI 44186) to J.M.B.

* To whom correspondence should be addressed. Telephone: (802) 656-8503. Fax: (802) 656-8749. E-mail: John.Burke@uvm.edu.

[1] Abbreviations: UV, ultraviolet; NMR, nuclear magnetic resonance; HEPES, *N*-(2-hydroxyethyl)piperazine-*N*′-2-ethanesulfonic acid; EDTA, ethylenediaminetetraacetic acid; dpm, disintegrations per minute.

10.1021/bi0028385 CCC: $20.00 © 2001 American Chemical Society
Published on Web 03/01/2001

potato spindle tuber viroid RNA and loop E from eukaryotic 5S ribosomal RNA (5S rRNA) (*16*). The consensus sequence has subsequently been identified in a number of other RNA internal or terminal loops and three-way helical junctions (*17*, *18*). In addition to the hairpin loop B structure, the eukaryotic loop E and 23S rRNA sarcin−ricin loop structures have been determined at atomic resolution (*17*, *19*, *20*). It is believed that this motif is particularly well suited to assembling higher-order structure by virtue of the abundance of accessible functional groups which line both the major and minor grooves (*21*). In the hairpin ribozyme, the motif is postulated to make an interaction with helix 2 of domain A during catalysis (*22*).

Lower-resolution methods such as fluorescence resonance energy transfer (FRET), photoaffinity cross-linking, and hydroxyl-radical footprinting have begun to shed light on the structure and dynamics of the docked complex (*23*−*25*). With these biochemical tools, we can now ask about the changes in the structures of the A and B domains that are brought about by docking. Several lines of evidence suggest that the organization of each domain undergoes significant rearrangement upon formation of the docked complex. First, a significant activation energy of docking, equal to 30 kcal/mol, has been observed using FRET and time-resolved footprinting (*23*; K. J. Hampel, and J. M. Burke, unpublished observations). This property is suggestive of a requirement for unfolding of an existing structure. Second, the loop A domain has recently been shown to undergo a significant structural change during catalysis as determined by photoaffinity cross-linking and activity assays (*45*). Third, nucleotide analogue interference modification (NAIM) analysis has demonstrated inconsistencies between the functional group requirements for ligation and the NMR structures of the isolated domains (*26*). The final point is of particular interest since the NAIM data predict that the UV sensitive substructure of loop B undergoes some rearrangement during catalysis. Here we provide direct evidence for a conformational change within this motif, using UV photo-cross-linking as a probe for local tertiary structure.

## MATERIALS AND METHODS

*Materials*. All RNAs were prepared by standard phosphoramidite chemistry from Glen Research. RNAs were deprotected and purified as described previously (*27*). RNA labeling at the 5′- and 3′-ends was performed using T4 polynucleotide kinase and RNA ligase, respectively, and the products were purified as described previously (*15*).

*Photo-Cross-Linking Experiments.* Ribozyme complexes were folded by mixing $2 \times 10^4$ dpm of 5′-$^{32}$P-end-labeled RNA with 250 nM unlabeled RNA components in a buffer containing 25 mM HEPES-NaOH (pH 7.5) with or without 12 mM $MgCl_2$ in a final volume of 10 $\mu$L. This mixture was pipetted into a well on a 96-well microtiter plate and irradiated with a portable 254 nm UV light (model UVG-54, UV Products Inc.; measured output, 2200 $\mu$W/cm$^2$) at a distance of 2 cm for 3 min at room temperature. RNA species were separated on 15% polyacrylamide (19:1 polyacrylamide:bisacylamide ratio), 8 M urea gels. Gel results were quantified using a Bio-Rad Molecular Imager System GS-525. Gel purification of cross-linked species and mapping of the sites of cross-linking were carried out as described previously (*15*, *25*).

Time-resolved cross-linking was carried out as follows. A 4 $\mu$L aliquot of an RNA mixture containing $5 \times 10^5$ dpm of [5′-$^{32}$P]RNA, 250 nM unlabeled RNAs, and 25 mM sodium cacodylate (pH 7.2) was pipetted into a well on a 96-well microtiter plate. An equal volume of a cation solution containing 24 mM $MgCl_2$ was added to the RNA solution. After a specific folding time at 21 °C, the plate was irradiated with UV light as described above for 10 s. A folding progress curve was calculated for all three data sets with Microcal Origin 4.1, using Marquardt−Levenberg nonlinear least-squares regression to the exponential association equation [$y = y_0 + A(1 - e^{-t/\tau})$].

*Self-Cleavage Kinetics of Cross-Linked Ribozymes*. A solution containing $1 \times 10^5$ dpm of 5′-$^{32}$P-labeled RNA, 250 nM cold RNA, 50 mM Tris-HCl (pH 7.5), and 0.1 mM EDTA (pH 8) was UV irradiated for 3 min. The irradiated sample was equilibrated at 25 °C for 5 min and then mixed with an equal volume of 24 mM $MgCl_2$ and 50 mM Tris-HCl (pH 7.5). Aliquots were removed from this mixture at various times and quenched into 5 volumes of 90% (v/v) formamide, 20 mM EDTA (pH 8), 0.02% (w/v) xylene cyanol, and 0.02% (w/v) bromophenol blue on ice. To provide a positive control for the gel mobility of self-cleaved, cross-linked RNA, 5′-$^{32}$P-labeled RNA was incubated with 0.5 $\mu$M unlabeled RNA in a buffer containing 12 mM $MgCl_2$ and 50 mM Tris-HCl (pH 7.5) at 25 °C for various times and then quenched into an equal volume of 20 mM EDTA. Quenched samples were irradiated for 3 min at room temperature.

*Native Gel Electrophoresis*. A saturating concentration of cold RNA (500 nM) and $1 \times 10^4$ dpm of 5′-$^{32}$P-end-labeled RNA or an equal number of counts of cross-linked RNAs was incubated in a folding buffer containing 40 mM Tris-acetate (pH 7.5), 25 mM $Mg^{2+}$-acetate, and 10% (v/v) glycerol for 10 min at 25 °C. This solution was then loaded onto a running 10% polyacrylamide gel and electrophoresed for 18 h at 4 °C. The gel buffers consisted of 40 mM Tris-acetate (pH 7.5), 25 mM $Mg^{2+}$-acetate (with $Mg^{2+}$ gel), or 40 mM Tris-acetate (pH 7.5), with 1 mM EDTA (without $Mg^{2+}$ gel).

*Time-Resolved Fe(II)-EDTA Footprinting.* A 4 $\mu$L aliquot of an RNA mixture containing $5 \times 10^5$ dpm of [5′-$^{32}$P]RNA, 250 nM unlabeled RNAs, and 25 mM sodium cacodylate (pH 7.2) was pipetted into a microfuge tube and incubated at 21 °C for 5 min. To the inside surface of this tube, near the bottom, were pipetted separate 0.7 $\mu$L aliquots of 0.35% (v/v) $H_2O_2$ (freshly prepared from a 30% v/v stock solution), 0.7 $\mu$L of 60 mM sodium ascorbate, and 0.7 $\mu$L of Fe(II)-EDTA [25 mM EDTA and 20 mM $Fe(NH_4)_2(SO_4)_2$ (mixed immediately prior to the experiment)]. To initiate RNA folding, 4 $\mu$L of a solution composed of 24 mM $MgCl_2$ and 25 mM sodium cacodylate (pH 7.2) (pre-equilibrated at 21 °C) was added to the RNA solution. After the prescribed folding time, hydroxyl-radical-generating reagents on the inside tube surface were introduced into the folding solution by gently flicking the bottom of the tube. After exposure for 3 s to hydroxyl radicals, this reaction was quenched by addition of 2 volumes of a solution containing 10 mM thiourea, 0.02% (v/v) bromphenol blue, and 0.02% (v/v) xylene cyanol in formamide. Reaction products were separated on 15% (w/v) acrylamide and 8 M urea gels.

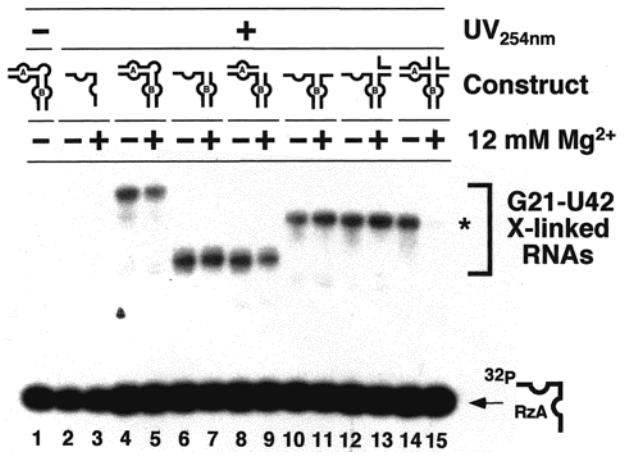


FIGURE 2: Docking of the A and B domains eliminates photosensitivity in loop B. End-labeled hairpin ribozyme−substrate constructs as shown were folded in a solution containing 50 mM HEPES-NaOH (pH 7.5) with or without 12 mM $Mg^{2+}$ for 10 min at 21 °C and then irradiated with 254 nm UV light for 3 min at room temperature. The G21−U42 cross-linked species are indicated with a bracket. The asterisk denotes the gel mobility of the G21−U42 cross-linked form that is lost upon folding of the 4WJ-SV5 construct. Samples were separated on a 15% polyacrylamide, 8 M urea gel and autoradiographed.

## RESULTS

Until recently, our studies of the structure of the hairpin ribozyme−substrate complex have been limited by the conformational heterogeneity exhibited by the wild-type sequence in the context of the minimal two-way interdomain junction (*11*, *29*; J. E. Heckman and J. M. Burke, unpublished observations). In particular, the docking equilibrium does not strongly favor the docked form in these constructs (K. J. Hampel and J. M. Burke, unpublished observations). Upon the design of a structurally well-behaved sequence variant, the SV5 ribozyme, it became possible to define, for example, a solvent-protected core between the A and B domains (*24*). This result prompted us to re-evaluate other structural studies originally carried out with the wild-type minimal ribozyme.

We first wished to study the impact of interdomain docking on the efficiency of formation of the UV cross-link between G21 and U42. To isolate the docking step from the subsequent cleavage step, the scissile bond is rendered uncleavable by a 2′-deoxy substitution of the −1 position. This modification does not negatively affect docking, and was used for all subsequent docking assays in this study (*23*). The UV-sensitive motif in loop B was not originally shown to be sensitive to conditions which promote interdomain docking, and catalysis (*15*). During a re-examination of this result, we observed that the level of the loop B cross-link was diminished when the A domain and $Mg^{2+}$ were both present, conditions required for docking (Figure 2). The bases involved in this cross-link were determined to be G21 and U42 for this and all subsequent experiments. To further test the impact of docking on the level of G21−U42 cross-linking, we examined this property in constructs which display different docking equilibria (Table 1 and Figure 2). The loss of the G21−U42 cross-link under ionic conditions which promote docking was in close agreement with the docked fraction determined by time-resolved FRET (trFRET) on identical constructs (*30*). The decrease in the level of cross-linking is particularly evident for the native four-way helical junction motif, where the fractional loss of cross-linking under docking conditions is 0.88 [Table 1 and Figure 2 (compare lanes 14 and 15)]. It is important to note that these experiments monitor only the fraction of molecules which become cross-linked (<5%) in each sample. In all of the constructs and mutants that we have studied, however, we find that the relative loss of the level of cross-linking is very similar to the fraction of molecules docked as observed by time-resolved FRET experiments (Table 1). It is unlikely that this is coincidental; therefore, we propose that when the molecule is in the docked conformation the photoreactivity of the loop E motif is significantly reduced.

Table 1: Fractional Loss of G21−U42 Cross-Linking during Docking, and Docking Distributions in Various Ribozyme−Substrate Complexes

| construct | modification | fractional loss of photosensitivity[a] | docked fraction by trFRET[b] |
|---|---|---|---|
| 2WJ-SV5 | none | 0.60 ± 0.04 | 0.74 ± 0.02 |
| 2WJ-SV5 | G+1/A | <0.02 | <0.02 |
| 2WJ-SV5 (without the $C_5$ linker) | none | 0.53 ± 0.05 | 0.65 ± 0.02 |
| 4WJ-SV5 | none | 0.88 ± 0.07 | 0.93 ± 0.01 |
| 4WJ-SV5 | G+1/A | 0.33 ± 0.05 | 0.39 ± 0.02 |

[a] Calculated from the equation $F = [XL^{Mg^{2+}}/(XL^{Mg^{2+}} + UXL^{Mg^{2+}})]/[XL/(XL + UXL)]$, where XL and UXL are the disintegrations per minute of cross-linked and un-cross-linked complexes, respectively. [b] From ref *30*.

Though we observed a strong correlation between the level of the docking and the magnitude of the loop B conformational change, in 2WJ-SV5 constructs the fraction of docked molecules is 1.2-fold higher than the loss in the level of cross-linking (Table 1). This discrepancy may indicate that a small fraction of docked molecules have not undergone the conformational change. Therefore, we wanted to assay for the presence of docked molecules which retain the photoreactive motif. The presence of a docked, cross-linked intermediate would support the proposal that the change in loop B structure occurs through an induced-fit mechanism. To address this question, we purified cross-linked RNAs and then subjected them to a nondenaturing gel electrophoresis protocol which differentiates the docked and undocked forms of the ribozyme−substrate complex. A clear electrophoretic discrimination between the docked and extended form requires an $AC_5$ linker between helix 3 and the substrate (data not shown). The G+1/A mutant served as a negative control for docking (*23*, *24*). In the presence of $Mg^{2+}$, this control complex runs as a single band with relatively low mobility (Figure 3, lane 4). The 2WJ-SV5 sequence resolves as two bands, a low-mobility band that comigrates with the G+1/A complex and a higher-mobility, compact form of greater abundance (Figure 3, lane 2). In the absence of $Mg^{2+}$, 2WJ-SV5 and the G+1/A variant comigrate as single bands. We conclude, therefore, that the upper and lower bands represent the undocked and docked forms, respectively. In this assay, we observe that 72 ± 6% of the 2WJ-SV5 complexes partition into the docked form, identical within error to that observed for the same construct in trFRET analysis (*30*). The purified cross-linked complexes had the mobility of the undocked control (Figure 3, lane 6). An irradiated but unpurified control was included to show that UV irradiation for 3 min does not cause sufficient damage

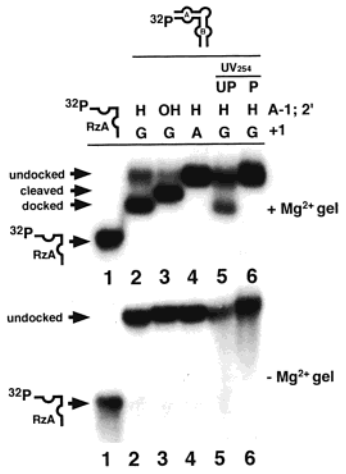


FIGURE 3: Nondenaturing gel electrophoresis of ribozymes shows that interdomain docking is disabled in G21−U42 cross-linked ribozymes. RNAs were incubated with 25 mM magnesium acetate, then diluted into an equal volume of the same buffer containing 20% (v/v) glycerol, and loaded onto a running 10% polyacrylamide gel in the presence (upper panel) or absence (lower panel) of 25 mM $Mg^{2+}$ as described in Materials and Methods. The +1 base identities and 2′-functional groups are indicated. UV-irradiated RNAs were employed either with (P) or without (UP) prior purification of the G21−U42 cross-linked complexes.

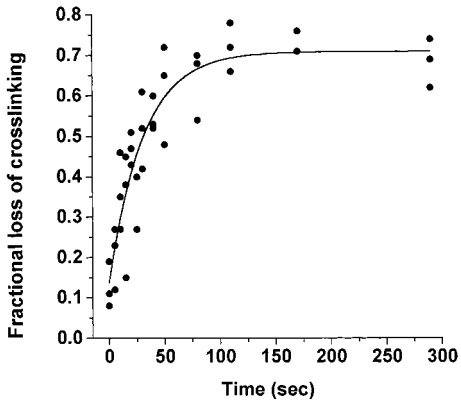


FIGURE 4: Loss of photosensitivity as a function of folding time. A mixture of 5′-end-labeled RzA and 250 $\mu$M 3′LB-S was was allowed to fold in a buffer containing 12 mM $Mg^{2+}$ at 21 °C for the indicated times and then irradiated with 254 nm UV light for 10 s. Irradiated RNAs were separated on a 15% polyacrylamide, 8 M urea gel, and the level of cross-linking was quantified by phosphorimager analysis. The loss in the level of cross-linking was determined by subtracting the fraction of G21−U42 cross-linked ribozyme−substrate complexes from that of identically treated constructs containing a docking mutation, G+1/A. The results of three replicate experiments are shown. A folding progress curve was calculated simultaneously for all three data sets with Microcal Origin 4.1, using Marquardt−Levenberg nonlinear least-squares regression to the exponential association equation [$y = y_0 + A(1 - e^{-t/\tau})$]. The resulting folding curves yielded a $k_{fold}$ of 1.94 ± 0.28 $min^{-1}$ and a maximum amplitude of 0.71 ± 0.04.

to entirely prevent docking (Figure 3, lane 5). We conclude that the G21−U42 cross-linked ribozyme−substrate complexes do not dock to a detectable extent. We also performed native gel analysis on a self-cleaving construct (Figure 3, lane 3). The self-cleaved form has a mobility distinct from those of the docked and undocked forms. This technique may thus be used to rapidly identify mutants that are compromised at some step after docking.

Our inability to observe a docked, photoreactive intermediate form may have been due to the instability of this form in the native gel system. We therefore determined the rate of the loss of cross-linking directly and compared this rate to the interdomain docking rate. It was possible to measure the kinetics of the conformational change since observable cross-linking of G21 and U42 occurs after exposure to 254 nm UV light for only 10 s (Figure 4). Folding of ribozyme−substrate complexes was initiated by the addition of 12 mM $Mg^{2+}$, and was allowed to continue for times between 0 and 300 s. The samples were then irradiated with UV light for 10 s to define the level of the conformational change. The rate of loss of the photoreactive structure after addition of $Mg^{2+}$ was 1.9 ± 0.3 $min^{-1}$. A newly developed time-resolved hyrodoxyl-radical footprinting method was used to define the docking rate for this construct (Figures 5 and 6) (*28*). The substrate positions surrounding the scissile bond, −2 to 2, and ribozyme positions 12−15, 25−27, 38, 42, and 43 become solvent-protected as a result of interdomain docking (*24*). To study the kinetics of internalizing these sites, folding of ribozyme−substrate complexes was initiated by addition of 12 mM $Mg^{2+}$. The extent of folding after specific folding times was monitored by a brief (3 s) exposure to hydroxyl radicals. An example of a gel result of this set of experiments is shown in Figure 5. A control complex that was incubated in the absence of $Mg^{2+}$ did not form a solvent-protected core after incubation for 10 min. When folded in 12 mM $Mg^{2+}$, ribozyme and substrate sites were protected with rates close to 2 $min^{-1}$ (Figure 6). Thus, to the precision of our measurements, the conformational change in loop B and docking occur on similar time scales.

Since docking is required for catalysis by the hairpin ribozyme, and disrupts the structure of the photoreactive loop E motif, we decided to re-examine the catalytic ability of cross-linked ribozymes. Previous results showed that the G21−U42 cross-linked ribozyme displayed weak trans-cleavage activity (*15*). This observation was interpreted as evidence for an essential role for the photoreactive local tertiary structure; however, the authors were not able to rule out the possibility that trans-cleavage activity could be attributed to a small quantity of un-cross-linked RNAs in their samples. In addition, it is now clear that in some mutants which are catalytically active, particularly those containing non-wild-type base pairs between positions +1 and 25, docking cannot be observed by FRET or native gel methods (*31*; K. J. Hampel and J. M. Burke, unpublished observations). Thus, we felt that it was important to re-examine the question of the catalytic activity of cross-linked ribozymes. Self-cleaving constructs can report directly on their ability to cleave RNA since the site of cross-linking is covalently linked to the substrate (*32*). Ribozyme-mediated cleavage, therefore, would produce a shortened, cross-linked complex that can be resolved electrophoretically. A control for the electrophoretic mobility of a G21−U42 self-cleaved construct was obtained by allowing a self-cleaving construct to react over a time course from 0 to 45 min in 12 mM $Mg^{2+}$, and then irradiating the resulting RNAs (Figure 7, left panel). For the experimental panel, the self-cleaving construct was cross-linked for 3 min and then allowed to self-cleave over the same time course (Figure 7, right panel). Cleavage products were observed for the RNAs that had not been cross-linked between G21 and U42, but no activity was

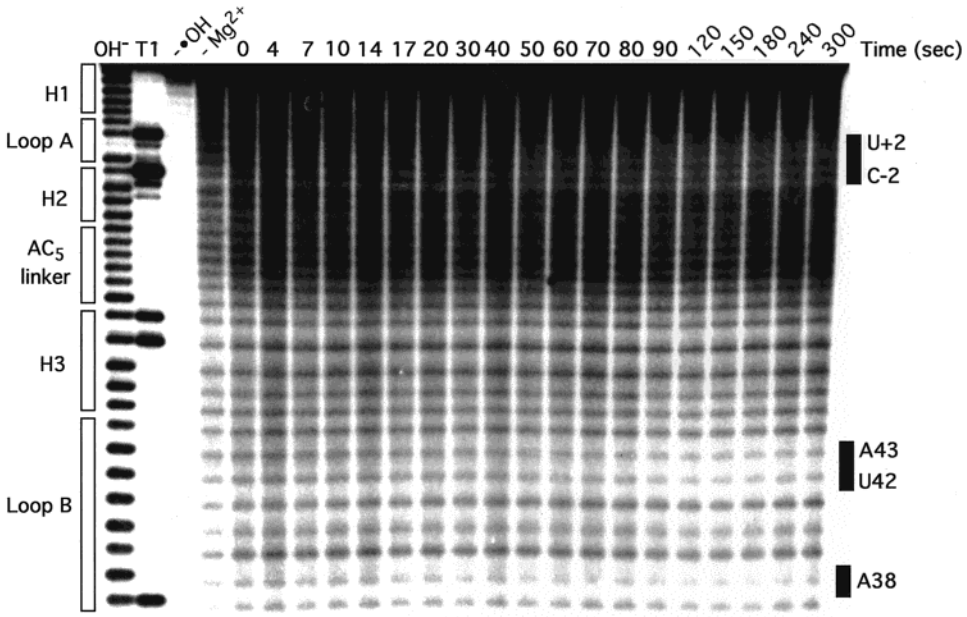


FIGURE 5: Folding kinetics determined by time-resolved hydroxyl-radical footprinting. An RNA solution containing 5′-end-labeled 3′LB-S and 0.25 $\mu$M RzA was folded in 12 mM $Mg^{2+}$ at 21 °C for the indicated folding times prior to 3 s of hydroxyl-radical-mediated cleavage. Reaction products were separated on a 15% (w/v) acrylamide, 8 M urea gel and autoradiographed. Sites that are protected by docking are indicated with black bars to the right of the gel. A negative control for docking, the $-Mg^{2+}$ lane, was incubated for 10 min at 21 °C prior to exposure to hydroxyl radicals. The sample in the −•OH lane was treated with hydroxyl radicals after addition of the quench solution. Note that the identity of each band on the Fe(II)-EDTA ladders is actually one nucleotide below the corresponding band on partial ribonuclease T1 and alkali hydrolysis ladders.

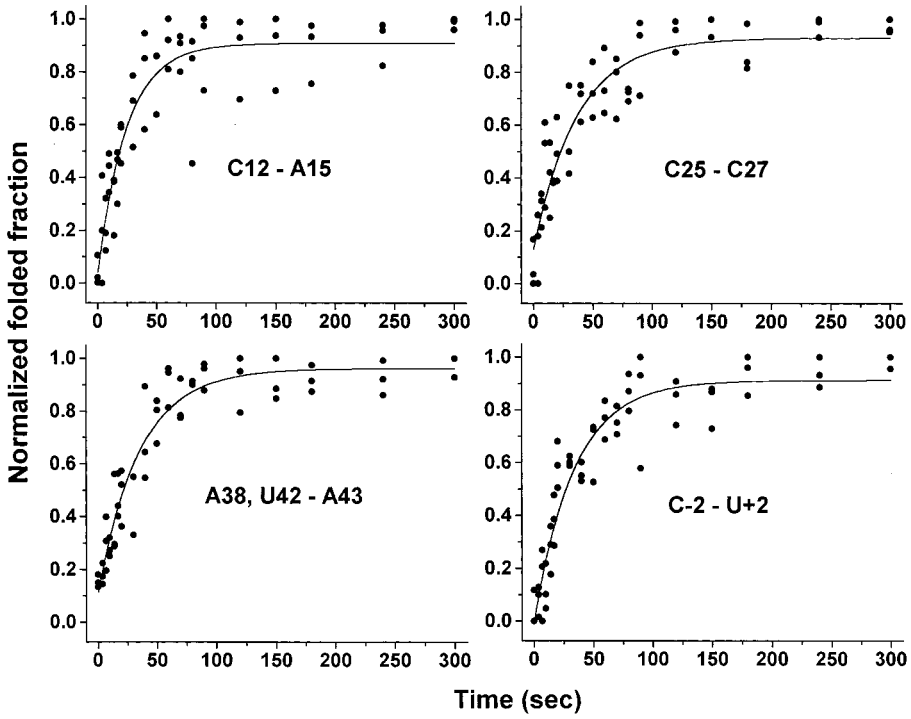


FIGURE 6: Quantification of time-resolved hydroxyl-radical footprinting results. Folding progress curves for each protected site in the ribozyme−substrate complex. To quantify protection at each time point, the number of counts in each lane at the protected site was subtracted from the same site on the −•OH lane. The number of counts at sites where the accessibility to hydroxyl-radical attack does not change upon formation of the docked complex were quantitated to correct for the lane-to-lane variation in gel loading and RNA cleavage. The results of three replicate experiments are shown. Each data set was normalized to the highest level of protection observed during that time course. Folding progress curves were calculated as described in the legend of Figure 4. The resulting folding curves yielded the following: $k_{fold}^{C12-A15} = 2.43 \pm 0.32$ min$^{-1}$, $k_{fold}^{A38,U42-A43} = 1.70 \pm 0.18$ min$^{-1}$, $k_{fold}^{C25-C27} = 1.63 \pm 0.22$ min$^{-1}$, and $k_{fold}^{C-2-U+2} = 1.77 \pm 0.19$ min$^{-1}$.

observed for cross-linked RNAs during 45 min at 25 °C as shown in Figure 3, or even after incubation for 4 h at 25 or 37 °C (data not shown). Thus, a ribozyme containing the G21−U42 cross-link is not catalytically active.

## DISCUSSION

We have identified a change in the structure of loop B that is induced by docking with the A domain. But, of what

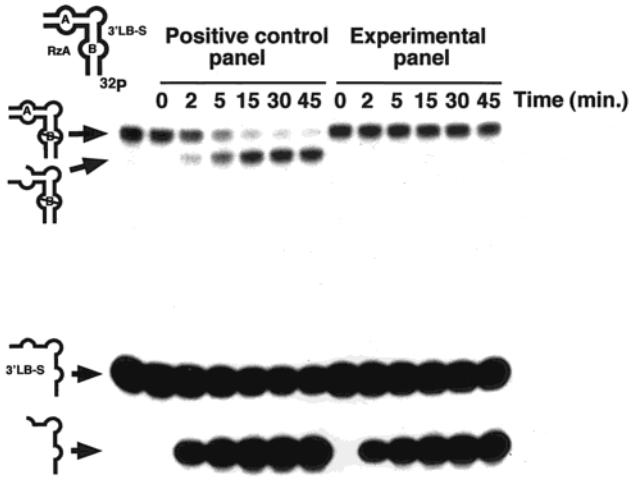


FIGURE 7: Cross-linked ribozymes are catalytically inactive. (Left) A control for the gel mobility of self-cleaved G21−U42 cross-linked RNA. 2WJ-SV5 was incubated in reaction buffer for the indicated times before quenching the self-cleavage reaction with EDTA. Samples were then irradiated with 254 nm UV light for 3 min on ice. (Right) Experimental panel demonstrating the lack of self-cleavage activity by G21−U42 cross-linked complexes. 2WJ-SV5 was irradiated with 254 nm UV light for 3 min on ice in the absence of $Mg^{2+}$. The pool of irradiated RNA was then incubated in reaction buffer for the indicated times at 25 °C. Reactions were quenched in 20 mM EDTA in gel loading buffer. Samples were separated on a 15% polyacrylamide, 8 M urea gel.

magnitude is this conformational change? The fraction of docked molecules at equilibrium is 1.2-fold higher than the loss in the level of cross-linking (Table 1). On the surface, this result suggests that the structural change is subtle and that our results represent a reduction in the cross-linking efficiency, not a complete loss of this characteristic. This interpretation, however, is correct only if it is assumed that docked molecules do not undock and become cross-linked during the 3 min irradiation time. The undocked form of loop B is cross-linked with a rate of ~1.7% $min^{-1}$ (data not shown). The undocking rate can be estimated to be 0.7 $min^{-1}$ given the docking rate for the 2WJ-SV5 construct, 2 $min^{-1}$, and the undocked ⇔ docked equilibrium from trFRET analysis, 2.8. Thus, on average, each docked molecule has undocked at least once during UV irradiation, and becomes highly susceptible to UV-induced cross-linking. This process removes molecules from the steady-state population and artificially inflates the apparent number of UV-reactive molecules at equilibrium. Further evidence of this effect comes from kinetic folding assays followed by UV cross-linking, where a very short 10 s irradiation was used (Figure 4). In this experiment, a fractional change in UV reactivity of 0.71 ± 0.07 was observed. This figure fits closely with the fraction of molecules that are docked as determined by trFRET and native gel analyses. Therefore, we infer that the conformational change upon docking eliminates the ability of G21 and U42 to form the photoreactive motif. This represents a significant change in the structure of loop B upon interaction with loop A. Why was this change in structure not observed in the earlier study? In that study, ribozyme−substrate complexes were irradiated for 30 min with the same light source and under conditions similar to those employed here (*15*). The combination of using a docking-deficient wild-type sequence and a prolonged period of irradiation is likely to have contributed to the failure to observe docking-dependent effects on the G21−U42 cross-link.

Our data show that the loop E-like tertiary motif is not involved in catalysis after completion of the interdomain docking event. The role that the motif plays during docking is unknown. Mutation and functional group substitution of the photoreactive structure results in a number of different catalytic phenotypes ranging from almost complete loss of function to gain of function (*7*, *22*, *26*, *33*−*36*). Although the structural consequences of several of these changes have been probed by photo-cross-linking, these studies show no clear correlation between the ability of the loop B to form a photoreactive tertiary structure and the ability of the ribozyme−substrate complex to catalyze cleavage and ligation reactions (*22*; K. J. Hampel and J. M. Burke, unpublished observations). Mutations that are expected to disrupt the UV-reactive structure can also be predicted on the basis of modeling studies and phylogenetic analysis of loop E family sequences (*37*). Kinetic studies of these mutants are likewise unable to provide clear conclusions about the importance of the tertiary structure (*22*). One hypothesis that has been advanced is that the loop E motif provides a part of the interface between the two domains during the initial interdomain contact and then undergoes an induced-fit structural change (*22*). This idea is supported by the finding that the effects of mutation at G21 can be suppressed by changing a U12•A−3 base pair in helix 2 to a C•G pair (*22*). Thus, structural changes to loop B can be accommodated by compensatory changes to its putative receptor in loop A. We obtained a negative result in our attempt to isolate a photoreactive loop B domain that is docked with loop A; thus, we are unable to find experimental support for an induced-fit docking mechanism.

An alternative hypothesis is that the loop E motif must undergo a rearrangement prior to any interaction with loop A. In this way, the stable loop E motif impedes docking by acting as a kinetic trap. The NMR study of loop B indicated that elements of the structure are dynamic (*14*). The sugar conformations for each loop residue were consistent with a range of puckers, and evidence was observed for a minor conformation where three pyrimidines (C25, U37, and U39) are bulged out of the loop to make way for purine-purine stacking. In addition, it was noted in the NMR study that the bulged U at position 41 of loop B is unlikely to provide stability to the motif afforded by the bulged G in the same position of the sarcin/ricin and eukaryotic loop E motifs. One of the roles for U41 may, therefore, be to contribute greater flexibility to the photoreactive motif and by doing so ensure that loop B is able to adopt an alternative conformation that is complementary to the tertiary structure of the A domain. The lack of an observable folding intermediate that retains the UV-reactive motif is consistent with this hypothesis, but does not positively assert its validity.

The loss of catalytic activity as a consequence of maintaining the cross-linkable structure warrants discussion. This result could be due to any one of three reasons. First, the cross-linked complexes may be catalytically inactive by virtue of their inability to form docked complexes as shown in Figure 3. This could be due to the structure of the cross-linking lesion itself or by constraining the structure of loop B in an inactive, trapped form as suggested above. It should be noted, however, that cross-linking lesions need not

interfere with the formation of structure. For example, ribozyme−substrate complexes that contain a UV-induced cross-link between G8 and A−1 in loop A retain catalytic activity (*45*). In addition, mutants that result in undetectable docking have previously been shown to retain significant catalytic activity (*31*; K. J. Hampel and J. M. Burke, unpublished observations).

Second, the G21−U42 lesion may prevent a specific conformational change that is required for catalysis. This idea is supported by our observation that the structure of the photoreactive motif changes upon docking (Figure 2). In addition, Ryder and Strobel have recently shown that ribozymes with 6-methyladenine modification of A43, a substitution that is expected to disrupt a G21−A43 sheared base pair within the photoreactive motif, were over-represented in an active selection pool (*26*). This result suggests that the loop E motif is disrupted during catalysis, a hypothesis that is strongly supported by the current study.

Finally, the formation of a G21−U42 cross-linked lesion in loop B could prohibit catalysis by changing essential elements of the active site. We believe that this is the least likely explanation since the photoreactive subdomain is distant from the active site of the ribozyme. Azidophenacyl cross-linking and hydroxyl-radical footprinting map the active site components to the helix 4-proximal region of loop B, and the observation of a Watson−Crick base pair between G+1 and C25 strongly supports this theory (*24*, *25*, *31*).

There are numerous examples of RNA structural changes which are induced by ligand or protein binding (*38*−*42*). While it is assumed that contacts between self-structured RNAs are often associated with similar changes in one or both molecules, there are relatively few examples of this due to the dearth of high-resolution structural data on multi-domain complexes, and their individual domain components (*43*). We are fortunate that high-resolution domain structures exist for the hairpin ribozyme, and that although no similar data exist for the docked form, we have developed the biochemical tools for probing the docked complex. Our data underscore the importance of using caution while interpreting the structures of isolated domains in terms of function, while supporting the need to gather such information.

## ACKNOWLEDGMENT

We are grateful to Dr. Bruno Sargueil and Dr. Joyce Heckman for critical reading of the manuscript.

## REFERENCES

1. Pan, J., and Woodson, S. A. (1998) *J. Mol. Biol. 280*, 597−609.
2. Wu, M., and Tinoco, I. (1998) *Proc. Natl. Acad. Sci. U.S.A. 95*, 11555−11560.
3. Treiber, D. K., and Williamson, J. R. (1999) *Curr. Opin. Struct. Biol. 9*, 339−345.
4. Andersen, A. A., and Collins, R. A. (2000) *Mol. Cell 5*, 469−478.
5. Buzayan, J. M., Gerlach, W. L., and Bruening, G. (1986) *Nature 323*, 349−353.
6. Walter, N. G., and Burke, J. M. (1998) *Curr. Opin. Chem. Biol. 2*, 24−30.
7. Fedor, M. J. (2000) *J. Mol. Biol. 297*, 269−291.
8. Hampel, A., and Tritz, R. (1989) *Biochemistry 28*, 4929−4933.
9. Feldstein, P. A., and Bruening, G. (1993) *Nucleic Acids Res. 21*, 1991−1998.
10. Komatsu, Y., Koizumi, I., Nakamura, H., and Ohtsuka, E. (1994) *J. Am. Chem. Soc. 116*, 3692−3696.
11. Butcher, S. E., Heckman, J. E., and Burke, J. M. (1995) *J. Biol. Chem. 270*, 29648−29651.
12. Murchie, A. I., Thomson, J. B., Walter, F., and Lilley, D. M. (1998) *Mol. Cell 1*, 873−881.
13. Cai, Z., and Tinoco, I. (1996) *Biochemistry 35*, 6026−6036.
14. Butcher, S. E., Allain, F. H.-T., and Feigon, J. (1999) *Nat. Struct. Biol. 6*, 212−216.
15. Butcher, S. E., and Burke, J. M. (1994) *Biochemistry 33*, 992−999.
16. Branch, A. D., Benenfeld, B. J., and Robertson, H. D. (1985) *Proc. Natl. Acad. Sci. U.S.A. 82*, 6590−6594.
17. Wimberly, B., Varani, G., and Tinoco, I. (1993) *Biochemistry 32*, 1078−1087.
18. Leontis, N. B., and Westhoff, E. (1998) *J. Mol. Biol. 283*, 571−583.
19. Szewczak, A. A., and Moore, P. B. (1995) *J. Mol. Biol. 247*, 81−98.
20. Correll, C. C., Munishkin, A., Chan, Y.-L., Ren, Z., Wool, I. G., and Steitz, T. A. (1998) *Proc. Natl. Acad. Sci. U.S.A. 95*, 13436−13441.
21. Wimberly, B. (1994) *Nat. Struct. Biol. 1*, 820−827.
22. Sargueil, B., McKenna, J., and Burke, J. M. (2000) *J. Biol. Chem.* (in press).
23. Walter, N. G., Hampel, K. J., Brown, K. M., and Burke, J. M. (1998) *EMBO J. 17*, 2378−2391.
24. Hampel, K. J., Walter, N. G., and Burke, J. M. (1998) *Biochemistry 37*, 14672−14682.
25. Pinard, R., Heckman, J. E., and Burke, J. M. (1999) *J. Mol. Biol. 287*, 239−251.
26. Ryder, S. P., and Strobel, S. A. (1999) *J. Mol. Biol. 291*, 295−311.
27. Walter, N. G., Yang, N., and Burke, J. M. (2000) *J. Mol. Biol. 298*, 539−555.
28. Hampel, K. J., and Burke, J. M. (2000) *Methods* (in press).
29. Esteban, J. A., Walter, N. G., Kotzorek, G., Heckman, J. E., and Burke, J. M. (1998) *Proc. Natl. Acad. Sci. U.S.A. 95*, 6091−6096.
30. Walter, N. G., Burke, J. M., and Millar, D. P. (1999) *Nat. Struct. Biol. 6*, 544−549.
31. Pinard, R., Lambert, D., Walter, N. G., Heckman, J. E., Major, F., and Burke, J. M. (1999) *Biochemistry 38*, 16035−16039.
32. Downs, W. D., and Cech, T. R. (1996) *RNA 2*, 718−732.
33. Siwkowski, A., Shippy, R., and Hampel, A. (1997) *Biochemistry 36*, 3930−3940.
34. Young, K. J., Vyle, J. S., Pickering, M. A., Cohen, M. A., Holmes, S. C., Merkel, O., and Grasby, J. A. (1999) *J. Mol. Biol. 288*, 853−866.
35. Grasby, J. A., Mersmann, K., Singh, M., and Gait, M. J. (1995) *Biochemistry 34*, 4068−4076.
36. Schmidt, S., Beigelman, L., Karpeisky, A., Usman, N., Sorensen, U. S., and Gait, M. J. (1996) *Nucleic Acids Res. 24*, 573−581.
37. Leontis, N. B., and Westhof, E. (1998) *RNA 4*, 1134−1153.
38. Ruff, M., Krishnaswamy, S., Boeglin, M., Poterszman, A., Mitschler, A., Podjarny, A., Rees, B., Thierry, J. C., and Moras, D. (1991) *Science 252*, 1682−1689.
39. Allain, F. H.-T., Gubser, C. C., Howe, P. W. A., Nagai, K., Neuhaus, D., and Varani, G. (1996) *Nature 380*, 646−650.
40. Peterson, R. D., and Feigon, J. (1996) *J. Mol. Biol. 264*, 863−877.
41. Dieckmann, T., Suzuki, E., Nakamura, G. K., and Feigon, J. (1996) *RNA 2*, 628−640.
42. Jiang, F., Kumar, R. A., Jones, R. A., and Patel, D. J. (1996) *Nature 382*, 183−186.
43. Butcher, S. E., Dieckmann, T., and Feigon, J. (1997) *EMBO J. 16*, 7490−7499.
44. Burke, J. M., Butcher, S. E., and Sargueil, B. (1996) in *Nucleic Acids and Molecular Biology* (Eckstein, F., and Lilley, D. M. J., Eds.) Vol. 10, pp 129−143, Springer-Verlag, Berlin.
45. Pinard, R., Lambert, D., Heckman, J. E., Esteban, J. A., Gundlach, C. W., IV, Hampel, K. J., Glick, G. D., Walter, N. G., Major, F., and Burke, J. M. (2001) *J. Mol. Biol.* (in press).

BI0028385